

June 24, 2018

# The $S_{E1}$ factor of radiative $\alpha$ capture on $^{12}\text{C}$ in cluster effective field theory

Shung-Ichi Ando<sup>1</sup>,

*School of Mechanical and ICT convergence engineering, Sunmoon University, Asan, Chungnam 31460, Republic of Korea*

The  $S_{E1}$ -factor of radiative  $\alpha$ -capture on  $^{12}\text{C}$  is studied in effective field theory. We discuss a modification of the counting rules for the radiative capture amplitudes and find two unfixed parameters remained in the amplitudes. Those two parameters are fitted to the experimental  $S_{E1}$  data, and an  $S_{E1}$  factor is obtained at the Gamow-peak energy as  $S_{E1} = 86 \pm 4 \text{ keV}\cdot\text{b}$ . We find that our result is in good agreement with previous estimates reported recently. We also discuss the uncertainty of the estimate in the present approach.

PACS(s): 11.10.Ef, 24.10.-i, 25.55.-e, 26.20.Fj

---

<sup>1</sup><mailto:sando@sunmoon.ac.kr>

## 1. Introduction

The radiative  $\alpha$  capture on carbon-12,  $^{12}C(\alpha, \gamma)^{16}O$ , is one of the fundamental reactions in nuclear-astrophysics, which determines the  $C/O$  ratio created in the stars [1]. The reaction rate, equivalently the astrophysical  $S$ -factor, of the process at the Gamow peak energy,  $E_G = 0.3$  MeV, however, cannot be determined in experiment due to the Coulomb barrier. It is necessary to employ a theoretical model to extrapolate the reaction rate down to  $E_G$  by fitting model parameters to experimental data typically measured at a few MeV.

In constructing a model for the study, one needs to take account of excited states of  $^{16}O$  [2], particularly, two excited bound states for  $l_{i-th}^\pi = 1_1^-$  and  $2_1^+$  just below the  $\alpha$ - $^{12}C$  breakup threshold at  $E = -0.045$  and  $-0.24$  MeV <sup>2</sup>, respectively, as well as two resonant (second excited)  $1_2^-$  and  $2_2^+$  states at  $E = 2.42$  and  $2.68$  MeV, respectively. The capture reaction to the ground state of  $^{16}O$  at  $E_G$  is expected to be  $E1$  and  $E2$  transition dominant due to the subthreshold  $1_1^-$  and  $2_1^+$  states, while the resonant  $1_2^-$  and  $2_2^+$  states play a dominant role in the available experimental data at low energies, typically  $1 \leq E \leq 3$  MeV. The main part of the  $S$ -factor, therefore, consists of  $S_{E1}$  and  $S_{E2}$  from the  $E1$  and  $E2$  transitions along with a small contribution,  $S_{casc}$ , from so called cascade transitions. During a last half century, a lot of experimental and theoretical studies for the reaction have been carried out. See Refs. [2, 3, 4, 5] for review.

Theoretical frameworks employed for the study are mainly categorized into two [5]: the cluster models using generalized coordinate method [6] or potential model [7] and the phenomenological models using the parameterization of Breit-Wigner,  $R$ -matrix [8], or  $K$ -matrix [9]. A recent trend of the study is to rely on intensive numerical analysis, in which a larger amount of the experimental data relevant to the study are accumulated, and a significant number of parameters of the models are fitted to the data by using computational power [5, 10, 11]. In the present work, to the contrary, we discuss another approach to estimate the  $S$ -factor at  $E_G$ ; we employ a new method for the study and discuss a calculation of the  $S_{E1}$  factor at  $E_G$  based on an effective field theory.

Effective field theories (EFTs) provide us a model independent and systematic method for theoretical calculations. An EFT for a system in question can be built by introducing a scale which separates relevant degrees of freedom at low energies from irrelevant ones at high energies. An effective Lagrangian is written down in terms of the relevant degrees of freedom and perturbatively expanded by counting the number of derivatives order by order. The irrelevant degrees of freedom are integrated out, and their effect is embedded in coefficients appearing in the Lagrangian. Thus, a transition amplitude is systematically calculated by writing down Feynman diagrams, while the coefficients appearing in the Lagrangian are fixed by experiment. For review, refer to Refs. [12, 13, 14, 15]. For last two decades, various processes essential in nuclear-astrophysics have been investigated by constructing EFTs:  $p(n, \gamma)d$  at BBN energies [16, 17] and  $pp$  fusion [18, 19, 20, 21],  $^3He(\alpha, \gamma)^7Be$  [22] and  $^7Be(p, \gamma)^7B$  [23, 24] in the Sun.

In the previous works [25, 26, 27], we have constructed an EFT of the radiative capture reaction,  $^{12}C(\alpha, \gamma)^{16}O$ , derived the counting rules for the reaction at  $E_G$ , and fitted some

---

<sup>2</sup>The energy  $E$  denotes that of the  $\alpha$ - $^{12}C$  system in center of mass frame.

parameters of the theory to the binding energies of the ground state and excited states,  $0_1^+, 0_2^+, 1_1^-, 2_1^+, 3_1^-$  ( $l_{i-th}^\pi$ ) states of  $^{16}\text{O}$  and the phase shift data of the elastic  $\alpha$ - $^{12}\text{C}$  scattering for  $l = 0, 1, 2, 3$  channels. (We review and discuss the counting rules for the radiative capture reaction in the following sections.) In the parameter fitting to the phase shift data, we have introduced resonance energies of  $^{16}\text{O}$  as a large scale of the theory. As suggested by Teichmann [28], below the resonance energies, the Breit-Wigner-type parameterization for resonances can be expanded in powers of the energy, and one can obtain an expression of the elastic scattering amplitude as the effective range expansion. In addition, we have included the effective range parameters up to third order ( $n = 3$  in powers of  $k^{2n}$ ) for the  $l = 0, 1, 2$  channels and up to fourth order ( $n = 4$ ) for the  $l = 3$  channel because of the modified counting rules discussed in Ref. [26]. Though the phase shift data below the resonance energies can be reproduced very well by using the fitted parameters, we find that significant uncertainties in the elastic scattering amplitudes are remained when interpolating them to  $E_G$ .

In the present work, we apply the calculation method of EFT to the study of the radiative capture process up to next-to leading order (NLO). Inclusion of the photon field into the present formalism is straightforward because a photon field abides in the covariant derivatives in the terms of the effective Lagrangian. In the standard counting rules, we approximately have three structures (momentum dependence) in the radiative capture amplitudes after fitting the effective range parameters to the phase shift data of the elastic scattering for  $l = 1$ . We discuss a modification of the standard counting rules because of an enhancement effect of the  $p$ -wave composite  $^{16}\text{O}$  propagator. After taking the modification into account, we have two structures, which are represented by two unknown constants, in the radiative capture amplitudes. The two constants are fitted to experimental  $S_{E1}$  data, and we calculate the  $S_{E1}$ -factor at  $E_G$ . A good agreement of our result with the other estimates reported recently is found. We also discuss the uncertainty of the result of the present work from the higher order terms of the theory.

The present paper is organized as follows: In section 2, the counting rules of EFT and the effective Lagrangian for the reactions are briefly reviewed, and the radiative capture amplitudes for the initial  $p$ -wave state and the formula of the  $S_{E1}$  factor are displayed in section 3. In section 4, a modification of the counting rules is discussed, and numerical results are presented in section 5. Finally, in section 6, results and discussion of the present work are presented.

## 2. Effective Lagrangian

In the study of the radiative capture process,  $^{12}\text{C}(\alpha, \gamma)^{16}\text{O}$ , at  $E_G = 0.3$  MeV employing an EFT, one may regard the ground states of  $\alpha$  and  $^{12}\text{C}$  as point-like particles whereas the first excited states of  $\alpha$  and  $^{12}\text{C}$  are chosen as irrelevant degrees of freedom, from which a large scale of the theory is determined [25]. Thus the expansion parameter of the theory is  $Q/\Lambda_H \sim 1/3$  where  $Q$  denotes a typical momentum scale  $Q \sim k_G$ ;  $k_G$  is the Gamow peak momentum,  $k_G = \sqrt{2\mu E_G} \simeq 41$  MeV, where  $\mu$  is the reduced mass of  $\alpha$  and  $^{12}\text{C}$ .  $\Lambda_H$  denotes a large momentum scale  $\Lambda_H \simeq \sqrt{2\mu_4 E_{(4)}} \text{ or } \sqrt{2\mu_{12} E_{(12)}} \sim 150$  MeV where  $\mu_4$  is the reduced mass of one and three-nucleon system and  $\mu_{12}$  is that of four and eight-

nucleon system.  $E_{(4)}$  and  $E_{(12)}$  are the first excited energies of  $\alpha$  and  $^{12}\text{C}$ , respectively. By including terms up to next-to-next-to-leading order, for example, one may have about 10% theoretical uncertainty for the amplitude.

An effective Lagrangian for the study of the radiative capture reaction may be written as [25, 29, 30, 31, 32]

$$\begin{aligned} \mathcal{L} = & \phi_\alpha^\dagger \left( iD_0 + \frac{\vec{D}^2}{2m_\alpha} + \dots \right) \phi_\alpha + \phi_C^\dagger \left( iD_0 + \frac{\vec{D}^2}{2m_C} + \dots \right) \phi_C \\ & + \sum_{n=0}^3 C_n^{(0)} d^\dagger \left[ iD_0 + \frac{\vec{D}^2}{2(m_\alpha + m_C)} \right]^n d - y^{(0)} \left[ d^\dagger (\phi_\alpha \phi_C) + (\phi_\alpha \phi_C)^\dagger d \right] \\ & + \sum_{n=0}^3 C_n^{(1)} d_i^\dagger \left[ iD_0 + \frac{\vec{D}^2}{2(m_\alpha + m_C)} \right]^n d_i - y^{(1)} \left[ d_i^\dagger (\phi_\alpha O_i^{(1)} \phi_C) + (\phi_\alpha O_i^{(1)} \phi_C)^\dagger d_i \right] \\ & - h^{(1)} \frac{y^{(0)} y^{(1)}}{\mu} \left[ (\mathcal{O}_i^{(1)} d)^\dagger d_i + \text{H.c.} \right] + \dots, \end{aligned} \quad (1)$$

where  $\phi_\alpha$  ( $m_\alpha$ ) and  $\phi_C$  ( $m_C$ ) are fields (masses) of  $\alpha$  and  $^{12}\text{C}$ , respectively.  $D^\mu$  is a covariant derivative,  $D^\mu = \partial^\mu + i\mathcal{Q}A^\mu$  where  $\mathcal{Q}$  is a charge operator and  $A^\mu$  is the photon field. The dots denote higher order terms.  $d$  and  $d_i$  are composite fields of  $^{16}\text{O}$  consisting of  $\alpha$  and  $^{12}\text{C}$  fields for  $l = 0$  and 1 channel, respectively. The operators for the  $l = 1$  channel are given as

$$O_l^{(1)} = i \left( \frac{\vec{D}_C}{m_C} - \frac{\vec{D}_\alpha}{m_\alpha} \right)_i, \quad \mathcal{O}_i^{(1)} = \frac{iD_i}{m_O}, \quad (2)$$

where  $m_O$  is the mass of  $^{16}\text{O}$  in ground state. The coupling constants,  $C_n^{(0)}$  and  $C_n^{(1)}$  with  $n = 0, 1, 2, 3$ , are fixed by using the effective range parameters of elastic  $\alpha$ - $^{12}\text{C}$  scattering for  $l = 0$  and 1 channel, respectively, while the coupling constants  $y^{(0)}$  and  $y^{(1)}$  are redundant; we set them as  $y^{(0)} = \sqrt{2\pi/\mu}$  and  $y^{(1)} = \sqrt{6\pi\mu}$ . A contact interaction, the  $h^{(1)}$  term, is introduced to renormalize divergence from loop diagrams. As we will discuss below, we find that two kinds of divergence, and thus we rewrite it as

$$h^{(1)} = g^{(1)} + pg^{(1)\prime}, \quad (3)$$

where  $p$  is the relative momentum of  $\alpha$ - $^{12}\text{C}$  system in the initial state. The two constants,  $g^{(1)}$  and  $g^{(1)\prime}$ , should be fixed by using experimental data.

### 3. Amplitudes and the $S_{E1}$ factor

In Fig. 1, diagrams for dressed composite propagators of  $^{16}\text{O}$  consisting of  $\alpha$  and  $^{12}\text{C}$  for  $l = 0$  and  $l = 1$  are depicted, in which the Coulomb interaction between  $\alpha$  and  $^{12}\text{C}$  is taken into account [25, 26]. In Fig. 2, diagrams of the radiative capture process from the initial  $l = 1$  state to the  $^{16}\text{O}$  ground ( $0_1^+$ ) state are depicted, in which the Coulomb interaction between  $\alpha$  and  $^{12}\text{C}$  is taken into account as well.

$$\text{---} \bullet \text{---} = \text{---} \text{---} + \text{---} \textcircled{---} \text{---} + \text{---} \textcircled{---} \textcircled{---} \text{---} + \dots$$

Figure 1: Diagrams for dressed  $^{16}\text{O}$  propagators. A thick (thin) dashed line represents a propagator of  $^{12}\text{C}$  ( $\alpha$ ), and a thick and thin double dashed line with and without a filled blob represent a dressed and bare  $^{16}\text{O}$  propagator, respectively. A shaded blob represents a set of diagrams consisting of all possible one-potential-photon-exchange diagrams up to infinite order and no potential-photon-exchange one.

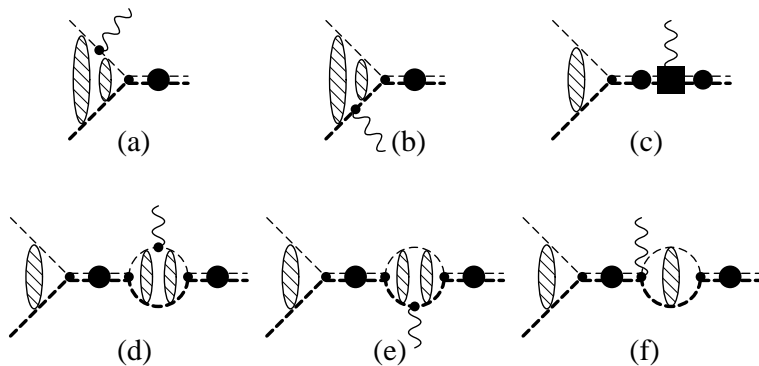


Figure 2: Diagrams for the radiative capture process from the initial  $p$ -wave  $\alpha$ - $^{12}\text{C}$  state. A wavy line denotes the outgoing photon, and the dressed composite propagator, whose diagrams are displayed in Fig. 1, in the final state denotes the ground ( $0_1^+$ ) state of  $^{16}\text{O}$ , and those in the intermediate state are the propagator for  $l = 1$  state. See the caption of Fig. 1 as well.

The radiative capture amplitude for the initial  $l = 1$  state is presented as

$$A^{(l=1)} = \bar{\epsilon}_{(\gamma)}^* \cdot \hat{p} X^{(l=1)}, \quad (4)$$

where  $\bar{\epsilon}_{(\gamma)}^*$  is the polarization vector of outgoing photon and  $\hat{p} = \vec{p}/|\vec{p}|$ ;  $\vec{p}$  is the relative momentum of the initial  $\alpha$  and  $^{12}\text{C}$ . The amplitude  $X^{(l=1)}$  can be decomposed as

$$X^{(l=1)} = X_{(a+b)}^{(l=1)} + X_{(c)}^{(l=1)} + X_{(d+e)}^{(l=1)} + X_{(f)}^{(l=1)}, \quad (5)$$

where those amplitudes correspond to the diagrams depicted in Fig. 2.

We follow the calculation method suggested by Ryberg *et al.* [33], in which Coulomb Green's functions are represented in coordinate space satisfying appropriate boundary conditions. Thus we obtain the expression of those amplitudes in center of mass frame as

$$\begin{aligned} X_{(a+b)}^{(l=1)} &= 2y^{(0)} \sqrt{Z_{gs}} e^{i\sigma_1} \Gamma(1 + \kappa/\gamma_0) \\ &\quad \times \int_0^\infty dr r W_{-\kappa/\gamma_0, \frac{1}{2}}(2\gamma_0 r) \left[ \frac{Z_\alpha \mu}{m_\alpha} j_0 \left( \frac{\mu}{m_\alpha} k' r \right) - \frac{Z_C \mu}{m_C} j_0 \left( \frac{\mu}{m_C} k' r \right) \right] \\ &\quad \times \left\{ \frac{\partial}{\partial r} \left[ \frac{F_1(\eta, pr)}{pr} \right] + 2 \frac{F_1(\eta, pr)}{pr^2} \right\}, \end{aligned} \quad (6)$$

$$X_{(c)}^{(l=1)} = +y^{(0)} (g^{(1)R} + pg^{(1)'}) \sqrt{Z_{gs}} \frac{6\pi Z_O}{\mu m_O} \frac{e^{i\sigma_1} p \sqrt{1 + \eta^2} C_\eta}{K_1(p) - 2\kappa H_1(p)}, \quad (7)$$

$$\begin{aligned} X_{(d+e)}^{(l=1)} &= +i \frac{2}{3} y^{(0)} \sqrt{Z_{gs}} \frac{e^{i\sigma_1} p^2 \sqrt{1 + \eta^2} C_\eta}{K_1(p) - 2\kappa H_1(p)} \Gamma(1 + \kappa/\gamma_0) \Gamma(2 + i\eta) \\ &\quad \times \int_{r_C}^\infty dr r W_{-\kappa/\gamma_0, \frac{1}{2}}(2\gamma_0 r) \left[ \frac{Z_\alpha \mu}{m_\alpha} j_0 \left( \frac{\mu}{m_\alpha} k' r \right) - \frac{Z_C \mu}{m_C} j_0 \left( \frac{\mu}{m_C} k' r \right) \right] \\ &\quad \times \left\{ \frac{\partial}{\partial r} \left[ \frac{W_{-i\eta, \frac{3}{2}}(-2ipr)}{r} \right] + 2 \frac{W_{-i\eta, \frac{3}{2}}(-2ipr)}{r^2} \right\}, \end{aligned} \quad (8)$$

$$X_{(f)}^{(l=1)} = -3y^{(0)} \sqrt{Z_{gs}} \mu [-2\kappa H(\eta_{b0})] \left( \frac{Z_\alpha}{m_\alpha} - \frac{Z_C}{m_C} \right) \frac{e^{i\sigma_1} p \sqrt{1 + \eta^2} C_\eta}{K_1(p) - 2\kappa H_1(p)}, \quad (9)$$

where  $k'$  is the magnitude of outgoing photon momentum.  $\kappa$  is the inverse of the Bohr radius,  $\kappa = Z_\alpha Z_C \mu \alpha_E$  where  $\alpha_E$  is the fine structure constant.  $Z_\alpha$ ,  $Z_C$ , and  $Z_O$  are the number of protons in  $\alpha$ ,  $^{12}\text{C}$  and  $^{16}\text{O}$ , respectively.  $\eta$  is the Sommerfeld parameter,  $\eta = \kappa/p$ , and  $\gamma_0$  is the binding momentum of the ground state of  $^{16}\text{O}$ ,  $\gamma_0 = \sqrt{2\mu B_0}$  where  $B_0$  is the binding energy compared to the  $\alpha$ - $^{12}\text{C}$  threshold energy.  $\Gamma(z)$  and  $j_l(x)$  are gamma function and spherical Bessel function, respectively, while  $F_l(\eta, \rho)$  and  $W_{k,\mu}(z)$  are regular Coulomb function and Whittaker function, respectively. In addition,

$$e^{i\sigma_1} = \sqrt{\frac{\Gamma(2 + i\eta)}{\Gamma(2 - i\eta)}}, \quad C_\eta^2 = \frac{2\pi\eta}{e^{2\pi\eta} - 1}, \quad H_1(p) = p^2(1 + \eta^2)H(\eta), \quad (10)$$

with

$$H(\eta) = \psi(i\eta) + \frac{1}{2i\eta} - \ln(i\eta), \quad (11)$$

where  $\psi(z)$  is digamma function.

The function  $K_1(p)$  contains the information about nuclear interaction and is represented in terms of the effective range parameters of the elastic  $\alpha$ - $^{12}\text{C}$  scattering for  $l = 1$  channel as <sup>3</sup>

$$K_1(p) = -\frac{1}{a_1} + \frac{1}{2}r_1p^2 - \frac{1}{4}P_1p^4 + Q_1p^6, \quad (12)$$

where  $a_1$  is fixed by using the binding energy of the  $1^-_1$  bound state of  $^{16}\text{O}$ , and other effective range parameters,  $r_1$ ,  $P_1$ , and  $Q_1$  are fitted to the experimental phase shift data. Furthermore,  $\sqrt{Z_{gs}}$  is wavefunction normalization constant of the ground state of  $^{16}\text{O}$ , which is obtained from the  $s$ -wave dressed  $^{16}\text{O}$  propagator as

$$D_O^{(l=0)}(p) = \frac{Z_{gs}}{E + B_0} + \dots, \quad (13)$$

where  $E$  is the total energy,  $E = p^2/(2\mu)$ , and the dots represent the terms regular at  $E = -B_0$  and

$$Z_{gs}^{-1} = \mu \left( r_0 + P_0 \gamma_0^2 + 6Q_0 \gamma_0^4 \right) - 2\kappa \frac{\mu\kappa}{\gamma_0^3} \left[ \psi^{(1)}(\kappa/\gamma_0) - \frac{\gamma_0^2}{2\kappa^2} - \frac{\gamma_0}{\kappa} \right], \quad (14)$$

where  $r_0$ ,  $P_0$ ,  $Q_0$  are effective range parameters;  $P_0$  and  $Q_0$  are fitted to the phase shift data of the elastic  $\alpha$ - $^{12}\text{C}$  scattering for  $l = 0$  channel, and  $r_0$  and the scattering length  $a_0$  are constrained by the binding energy of  $0^+_1$  and  $0^+_2$  states of  $^{16}\text{O}$ .  $\psi^{(n)}(z)$  is a polygamma function. We, thus, have obtained  $\sqrt{Z_{gs}} = 7.38$  [27]. In the present approach, the ground state of  $^{16}\text{O}$  consists of only  $\alpha$  and  $^{12}\text{C}$ , however, the real ground state of  $^{16}\text{O}$  contains other configurations of the nucleons. Thus we introduce a free (dimensionless) parameter  $C$  in the total cross section, which could be associated with a portion of the  $\alpha$ - $^{12}\text{C}$  configuration in the ground state of  $^{16}\text{O}$  for the present formalism and is fitted to the experimental  $S_{E1}$  data below.

Regarding the divergence from the loop diagrams, the loops of the diagrams (a) and (b) in Fig. 2 are finite, while those of the diagrams (d) and (e) lead to a log divergence in  $X_{(d+e)}^{(l=1)}$  in the limit,  $r \rightarrow 0$ . We thus introduce a short range cutoff  $r_C$  in the  $r$  integral in Eq. (8), and the divergence is renormalized by the counter term  $g^{(1)'} \psi^{(1)}$  introduced in Eq. (3). The loop of the diagram (f) diverges as well and is renormalized by a counter term, the  $g^{(1)}$  term in Eq. (3) as

$$g^{(1)R} = g^{(1)} - \mu \frac{m_O}{Z_O} \left( \frac{Z_\alpha}{m_\alpha} - \frac{Z_C}{m_C} \right) J_0^{div.}, \quad (15)$$

with

$$J_0^{div.} = \frac{\kappa\mu}{2\pi} \left[ \frac{1}{\epsilon} - 3C_E + 2 + \ln \left( \frac{\pi\mu_{DR}^2}{4\kappa^2} \right) \right], \quad (16)$$

---

<sup>3</sup>In the previous work, we had used another parameterization, so called  $v$ -parameterization, to represent the effective range parameters [34].

where we have used the dimensional regularization in  $4 - 2\epsilon$  space-time dimensions;  $C_E = 0.577\cdots$ , and  $\mu_{DR}$  is the scale from the dimensional regularization.  $g^{(1)R}$  is the renormalized coupling which should be fixed by experiment. In addition, the finite term  $-2\kappa H(\eta_{b0})$  in  $X_{(f)}^{(l=1)}$  from the loop of the diagram (f) where  $\eta_{b0} = \kappa/(i\gamma_0)$  is a quantity of a typical scale,  $-2\kappa H(\eta_{b0}) = 25.8$  MeV.

The  $S_{E1}$ -factor is defined by

$$S_{E1}(E) = \sigma_{E1}(E)Ee^{2\pi\eta}, \quad (17)$$

where the total cross section is

$$\sigma_{E1}(E) = \frac{4}{3} \frac{\alpha_E \mu E'_\gamma}{p(1 + E'_\gamma/m_O)} |X^{(l=1)}|^2 C, \quad (18)$$

with

$$E'_\gamma \simeq B_0 + E - \frac{1}{2m_O} (B_0 + E)^2. \quad (19)$$

#### 4. Modification of the counting rules

Before fitting the parameters to available experimental data, we discuss modification of the counting rules for the radiative capture amplitudes. An order of an amplitude is found by counting the number of momenta of vertices and propagators in Feynman diagrams. Thus one has a leading order (LO) amplitude from the  $g^{(1)R}$  term of the diagram (c) because the contact  $\gamma$ - $d$ - $d$  vertex itself does not have a momentum dependence, and NLO amplitudes from the other diagrams in Fig. 2 when using the standard counting rules. One may notice a large suppression factor,  $Z_\alpha/m_\alpha - Z_C/m_C$ , appearing in  $X_{(f)}^{(l=1)}$ ;  $(m_O/Z_O)(Z_\alpha/m_\alpha - Z_C/m_C) \simeq -6.5 \times 10^{-4}$ . Similar suppression effect can be found in  $X_{(a+b)}^{(l=1)}$  and  $X_{(d+e)}^{(l=1)}$  as well: we denote those amplitudes as  $X^-$ , and when changing the minus sign to the plus one in the front of the spherical Bessel function  $j_0(z)$  in Eqs. (6) and (8), we do them as  $X^+$ . We thus have  $|X_{(a+b)}^{(l=1)-}/X_{(a+b)}^{(l=1)+}| \simeq 8.7 \times 10^{-4}$  and  $|X_{(d+e)}^{(l=1)-}/X_{(d+e)}^{(l=1)+}| \simeq 3.6 \times 10^{-4}$  at the energy range,  $E = 0.9 - 3$  MeV, at which we fit the parameters to the experimental  $S_{E1}$  data in the next section. The suppression effect is common among those amplitudes, thus it does not alter the order counting of the diagrams.

We now discuss an enhancement effect which modifies the counting rules for the amplitudes due to the  $p$ -wave dressed  $^{16}\text{O}$  propagator in the diagrams (c), (d), (e), and (f). The  $p$ -wave dressed  $^{16}\text{O}$  propagator is enhanced due to large cancellations between the effective range terms and terms generated from the Coulomb self-energy term  $H_1(p)$ , as discuss in Ref. [26]. In the standard counting rules it is assigned to  $Q^{-3}$ , while because of the inclusion up to the  $Q_1 p^6$  term in the effective range expansion it should be counted as  $Q^{-9}$ . To check the magnitude of the enhancement effect, we calculate a ratio of the amplitudes,  $|X_{(f)}^{(l=1)}/X_{(a+b)}^{(l=1)}| \simeq 1.2 \times 10^3 - 6.7 \times 10^3$  at  $E = 0.9 - 3$  MeV, in which no free parameter is involved. Thus the contribution from the non-pole amplitude  $X_{(a+b)}^{(l=1)}$ , which does not have the  $p$ -wave dressed  $^{16}\text{O}$  propagator, is negligible in the present study.

In summary, after taking the enhancement effect into account, we have the  $g^{(1)R}$  term from  $X_{(c)}^{(l=1)}$  at LO, and the counter term  $g^{(1)'}$  from  $X_{(c)}^{(l=1)}$ ,  $X_{(d+e)}^{(l=1)}$ , and  $X_{(f)}^{(l=1)}$  at NLO, and  $X_{(a+b)}^{(l=1)}$  at a higher order. One may now see approximately two structures (momentum dependence) are remained among those amplitudes. One is the terms consist of the  $g^{(1)R}$  term from  $X_{(c)}^{(l=1)}$  and  $X_{(f)}^{(l=1)}$ , and the other does of the  $g^{(1)'}$  term from  $X_{(c)}^{(l=1)}$  and  $X_{(d+e)}^{(l=1)}$ , which contain an additional momentum  $p$  dependence to the first ones. The third structure of the amplitude is the non-pole one,  $X_{(a+b)}^{(l=1)}$ , but it turns out to be negligible in the modified counting rules. We have two parameters,  $g^{(1)R}$  and  $g^{(1)'}$ , in each of those two structures of the amplitudes, while there is an overall constant  $C$  in the total cross section. Thus one of the three parameters,  $g^{(1)R}$ ,  $g^{(1)'}$  and  $C$ , becomes redundant in the parameter fitting. In the present work, we choose  $g^{(1)R} = 0$  and fit the other two parameters,  $g^{(1)'}$  and  $C$ , to the data.

## 5. Numerical results

We have five parameters to fit to the data in the radiative capture amplitudes; three parameters,  $r_1$ ,  $P_1$ ,  $Q_1$ , are fitted to phase shift data and other two parameters,  $g^{(1)'}$  and  $C$  are to the experimental  $S_{E1}$  data. The standard  $\chi^2$ -fit is performed by employing a Markov chain Monte Carlo method for the parameter fitting.<sup>4</sup> The phase shift data for  $l = 1$  channel are taken from Tischhauser *et al.*'s paper [36], and the experimental  $S_{E1}$  data are from the literature [37, 38, 39, 40, 41, 42, 43, 44, 45] summarized in Tables V and VII in Ref. [5].

We fit the effective range parameters to the phase shift data for  $l = 1$  at  $E_\alpha = 2.6 - 6.0$  MeV and have

$$r_1 = 0.415255(9) \text{ fm}^{-1}, \quad P_1 = -0.57484(9) \text{ fm}, \quad Q_1 = 0.02016(2) \text{ fm}^3, \quad (20)$$

where the number of the data is  $N = 273$  and  $\chi^2 = 504$ , and thus  $\chi^2/N = 1.85$ . The uncertainties of the fitted values stem from those of the experimental data. The scattering volume  $a_1$  is fixed by using the condition that the denominator of the elastic scattering amplitude vanishes at the binding energy of the  $1_1^-$  state,  $E = -0.045$  MeV. Using the relation in Eq. (6) in Ref. [26] and the fitted effective range parameters we have

$$a_1 = -1.67 \times 10^5 \text{ fm}^3. \quad (21)$$

In Fig. 3, we plot a curve of the phase shift  $\delta_1$  calculated by using the fitted effective range parameters as a function of  $E_\alpha$ , where  $E_\alpha$  is the  $\alpha$  energy in lab frame<sup>5</sup>. We include the experimental data in the figure as well. One can see that the theory curve well reproduces the experimental data at the energy range,  $E_\alpha = 2.5 - 6.0$  MeV. Because the energy range is over the energy of  $1_2^-$  state,  $E = 2.43$  MeV ( $E_\alpha = 3.23$  MeV) and below that of  $1_3^-$  state,  $E = 5.29$  MeV ( $E_\alpha = 7.05$  MeV), our result indicates that the expression of the effective range expansion given in Eq. (12) is reliable to describe the  $1_1^-$  and  $1_2^-$  states up to  $E_\alpha = 6.0$  MeV.

---

<sup>4</sup>We employ a python package, `emcee`[35], for the fitting.

<sup>5</sup>The center of mass energy  $E$  is related to  $E_\alpha$  by  $E_\alpha \simeq \frac{4}{3}E$ .

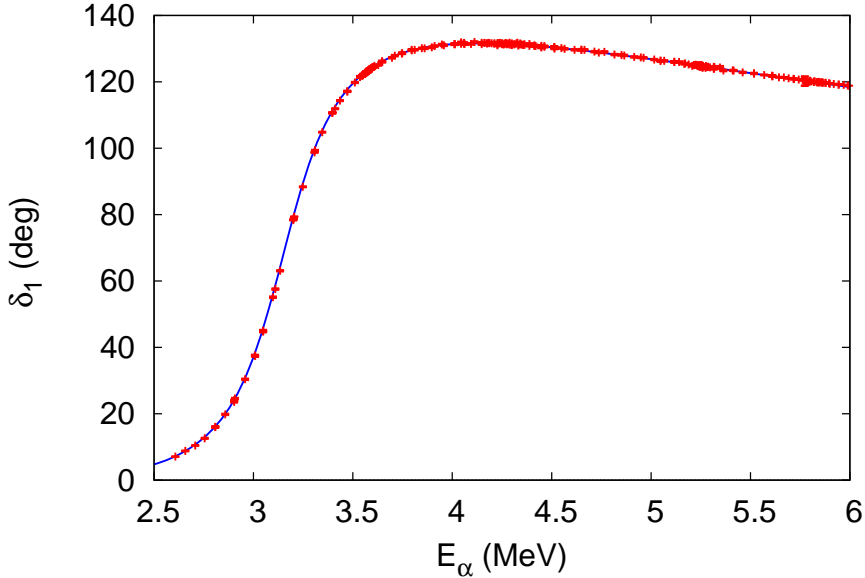


Figure 3: Phase shift,  $\delta_1$ , plotted by using the fitted effective range parameters,  $r_1$ ,  $P_1$ ,  $Q_1$  as a function of  $E_\alpha$ . The experimental phase shift data are also displayed in the figure.

We fit the parameters,  $g^{(1)'} \text{ and } C$  to the experimental  $S_{E1}$  data at the energy range,  $E = 0.9 - 3.0$  MeV and have

$$g^{(1)'} = -94.2(13) \text{ MeV}^2, \quad C = 2.04(9) \times 10^{-2}, \quad (22)$$

where  $N = 151$  and  $\chi^2 = 248$ , and thus  $\chi^2/N = 1.64$ . The uncertainties of the fitted values stem from those of the experimental data. We have used the short range cutoff,  $r_C = 0.35$  fm, in the  $r$  integral in  $X_{(d+e)}^{(l=1)}$  in Eq. (8). We find a mild cutoff dependence of the  $S_{E1}$  factor in the numerical result when varying the short range cutoff,  $r_C = 0.01 - 1$  fm. In Fig. 4, we plot a curve of  $S_{E1}$  calculated by using the fitted parameters. We include the experimental data in the figure as well. One can see that the theory curve reproduces well the experimental data.

At the Gamow-peak energy,  $E_G = 0.3$  MeV, thus, we have

$$S_{E1} = 86 \pm 4 \text{ keV}\cdot\text{b}, \quad (23)$$

where the small, about 5%, uncertainty stems from those of  $g^{(1)'} \text{ and } C$  in Eq. (22). The previous estimates of the  $S_{E1}$  factor at  $E_G$  are summarized in Table IV in Ref. [5]. The reported values are scattered from 1 to 340 keV·b with various size of the error bars. Nonetheless it is remarkable that our result is in good agreement with those reported recently:  $86 \pm 22$  by Tang *et al.* (2010) [46], 83.4 by Schurmann *et al.* (2012) [47],

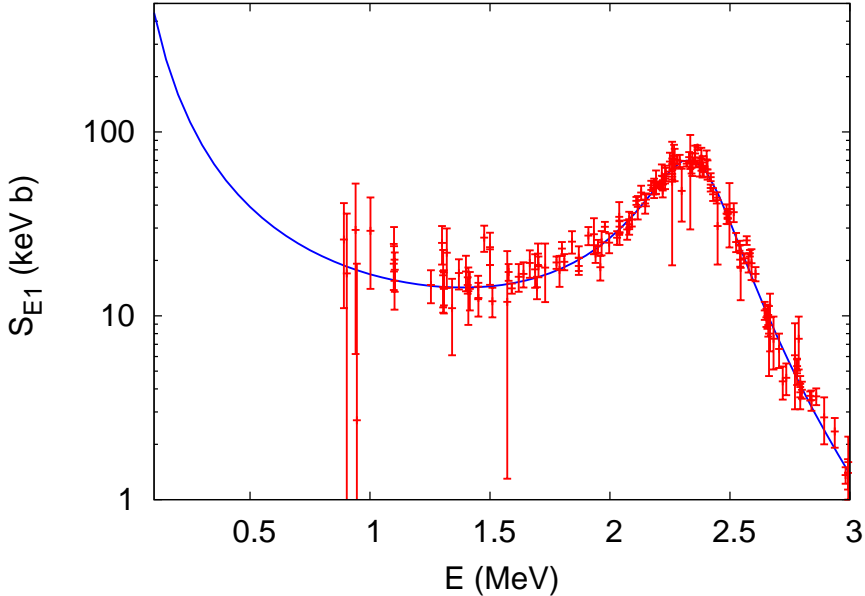


Figure 4:  $S_{E1}$  factor plotted by using the fitted parameters as a function of  $E$ . The experimental data are also displayed in the figure.

$100 \pm 28$  by Oulebsir *et al* (2012) [48],  $80 \pm 18$  by Xu *et al.* (2013) [10],  $98.0 \pm 7.0$  by An *et al.* (2015) [11], and  $86.3$  by dwBoer *et al.* (2017) [5].

Regarding the convergence of the expansion series of the theory, because we have chosen  $g^{(1)R} = 0$ , which is the coefficient of the only LO term,  $X_{(c)}^{(l=1)}$ , in the present study, all of the remaining amplitudes are at the same order, NLO (and the non-pole amplitude  $X_{(a+b)}^{(l=1)}$  is highly suppressed). Thus we cannot examine a convergence of the expansion series expected by the theory. A higher order correction will give about  $1/3$  correction to the amplitude. Thus, though a correction from the higher orders is re-fitted and the total amplitude is normalized to the experimental data available at a few MeV, one can expect that such a correction will lead to not tiny effect to the quantity at  $E_G$ .

## 6. Results and discussion

In this work, we have applied a framework of EFT to the study of radiative  $\alpha$  capture on  $^{12}\text{C}$ . We have derived the radiative capture amplitudes up to NLO in the standard counting rules, and discussed a modification of the counting rules for the radiative capture amplitudes because of the enhancement of the  $p$ -wave dressed composite propagator of  $^{16}\text{O}$ . We find that the non-pole amplitude  $X_{(a+b)}^{(l=1)}$  becomes negligible in the present study. After taking the modification into account, approximately two independent structures (momentum dependence) are remained in the amplitudes, and we assign two parameters to those two structures. The two parameters are fitted to the experimental  $S_{E1}$  data at  $E = 0.9 - 3.0$  MeV, and we find the  $S_{E1}$  factor,  $S_{E1} = 86 \pm 4$  keV·b at  $E_G$ . The result is

in good agreement with the estimates reported recently, though we have not examined a theoretical uncertainty in our result yet.

A unique feature of EFT is that one can control a theoretical uncertainty of a physical quantity in the theory. In the present work, however, we cannot examine a theoretical uncertainty in the estimate of the  $S_{E1}$  factor. Thus it is important to study higher order corrections to the radiative capture amplitude at next-to-next-to-leading order (NNLO) to check the convergence of the expansion series and estimate a theoretical uncertainty. It may not be easy, nonetheless, to accurately fix additional parameters due to the present quality of the experimental data set of  $S_{E1}$  when one includes higher order terms. Thus it may be better studying the other quantities at low energies, such as the  $\beta$ -delayed  $\alpha$  emission spectrum of  $^{16}\text{N}$  or the  $\gamma$  angular distribution of the radiative  $\alpha$  capture process by employing the present EFT approach.

### Acknowledgements

The author would like to thank Kyungsik Kim, Young-Ho Song, and Youngman Kim for useful discussion. This work was supported by the Basic Science Research Program through the National Research Foundation of Korea funded by the Ministry of Education of Korea (Grant No. NRF-2016R1D1A1B03930122) and in part by the National Research Foundation of Korea (NRF) grant funded by the Korean government (Grant No. NRF-2016K1A3A7A09005580).

## References

- [1] W.A. Fowler, Rev. Mod. Phys. **56**, 149 (1984).
- [2] L.R. Buchmann and C.A. Barnes, Nucl. Phys. A **777**, 254 (2006).
- [3] A. Coc, F. Hammache, J. Kiener, Eur. Phys. J. A **51**, 34 (2015).
- [4] C.A. Bertulani and T. Kajino, Prog. Part. Nucl. Phys. **89**, 56 (2016).
- [5] R.J. deBoer *et al.*, Rev. Mod. Phys. **89**, 035007 (2017), and references therein.
- [6] P. Descouvemont, D. Baye, and P.-H. Heenen, Nucl. Phys. A **430**, 426 (1984).
- [7] K. Langanke and S.E. Koonin, Nucl. Phys. A **439**, 384 (1985).
- [8] A.M. Lane and R.G. Thomas, Rev. Mod. Phys. **30**, 257 (1958).
- [9] J. Humblet, P. Dyer, and B.A. Zimmerman, Nucl. Phys. A **271**, 210 (1976).
- [10] Y. Xu *et al.*, Nucl. Phys. A **918**, 61 (2013).
- [11] Z.-D. An *et al.*, Phys. Rev. C **92**, 045802 (2015).
- [12] P.F. Bedaque and U. van Kolck, Ann. Rev. Nucl. Part. Sci. **52**, 339 (2002).

- [13] E. Braaten and H.-W. Hammer, Phys. Rept. **428**, 259 (2006).
- [14] U.-G. Meißner, Phys. Scripta **91**, 033005 (2016).
- [15] H.-W. Hammer, C. Ji, D.R. Phillips, J. Phys. G **44**, 103002 (2017).
- [16] G. Rupak, Nucl. Phys. A **678**, 405 (2000).
- [17] S. Ando, R.H. Cyburt, S.W. Hong, C.H. Hyun, Phys. Rev. C **74**, 025809 (2006).
- [18] X. Kong and F. Ravndal, Nucl. Phys. A **656**, 421 (1999).
- [19] M. Butler, J.-W. Chen, Phys. Lett. B **520**, 87 (2001).
- [20] S. Ando, J.W. Shin, C.H. Hyun, S.W. Hong, K. Kubodera, Phys. Lett. B **668**, 187 (2008).
- [21] J.-W. Chen, C.-P. Liu, S.-H. Yu, Phys. Lett. B **720**, 385 (2013).
- [22] R. Higa, G. Rupak, A. Vaghani, Eur. Phys. J. A **54**, 89 (2018).
- [23] X. Zhang, K.M. Nollett, and D.R. Phillips, Phys. Rev. C **89**, 051602(R) (2014).
- [24] E. Ryberg, C. Forssen, H.-W. Hammer, L. Platter, Eur. Phys. J. A **50**, 170 (2014).
- [25] S.-I. Ando, Eur. Phys. J. A **52**, 130 (2016).
- [26] S.-I. Ando, Phys. Rev. C **97**, 014604 (2018).
- [27] S.-I. Ando, work submitted to J. Korean Phys. Soc.
- [28] T. Teichmann, Phys. Rev. **83**, 141 (1951).
- [29] S.R. Beane, M.J. Savage, Nucl. Phys. A **694**, 511 (2001).
- [30] S. Ando, C.H. Hyun, Phys. Rev. C **72**, 014008 (2005).
- [31] S. Ando, J.W. Shin, C.H. Hyun, S.W. Hong, Phys. Rev. C **76**, 064001 (2007).
- [32] S.-I. Ando, Eur. Phys. J. A **33**, 185 (2007).
- [33] E. Ryberg, C. Forssen, H.-W. Hammer, and L. Platter, Phys. Rev. C **89**, 014325 (2014).
- [34] S.-I. Ando and C.H. Hyun, Phys. Rev. C **86**, 024002 (2012).
- [35] D. Foreman-Mackey *et al.*, arXiv:1202.3665v4 [astro-ph.IM] (2013).
- [36] P. Tischhauser *et al.*, Phys. Rev. C **79**, 055803 (2009).
- [37] P. Dyer and C. Barnes, Nucl. Phys. A **233**, 495 (1974).

- [38] A. Redder *et al.*, Nucl. Phys. A **462**, 385 (1987).
- [39] J.M.L. Ouellet *et al.*, Phys. Rev. C **54**, 1982 (1996).
- [40] G. Roters *et al.*, Eur. Phys. J. A **6**, 451 (1999).
- [41] L. Gialanella *et al.*, Eur. Phys. J. A **11**, 357 (2001).
- [42] R. Kunz *et al.*, Phys. Rev. Lett. **86**, 3244 (2001).
- [43] M. Fey, Ph.D. thesis (Universitat Stuttgart) (2004).
- [44] H. Makii *et al.*, Phys. Rev. C **80**, 065802 (2009).
- [45] R. Plag *et al.*, Phys. Rev. C **86**, 015805 (2012).
- [46] X.D. Tang *et al.*, Phys. Rev. C **81**, 045809 (2010).
- [47] D. Schurmann *et al.*, Phys. Lett. B **711**, 35 (2012).
- [48] N. Oulebsir *et al.*, Phys. Rev. C **85**, 035804 (2012).